

Interlayer decoupling in twisted bilayers of β -phosphorus and arsenic: a computational study

Shantanu Agnihotri,¹ Maneesh Kumar,² Yogesh Singh Chauhan,¹ Amit Agarwal,³ and Somnath Bhowmick^{2,*}

¹*Department of Electrical Engineering, Indian Institute of Technology Kanpur, Kanpur, U.P., 208016, India*

²*Department of Materials Science and Engineering,
Indian Institute of Technology Kanpur, Kanpur, U.P., 208016, India*

³*Department of Physics, Indian Institute of Technology Kanpur, Kanpur, U.P., 208016, India*

(Dated: May 16, 2019)

We investigate magnetism and band structure engineering in Moiré superlattice of blue phosphorus (β -P) and grey arsenene (β -As) bilayers, using *ab initio* calculations. The electronic states near the valence and conduction band edges have significant p_z character in both the bilayers. Thus, twisting the layers significantly reduce the interlayer orbital overlap, leading to a decrease in the binding energy (up to $\sim 33\%$) and an increase in interlayer distance (up to $\sim 10\%$), compared to the most stable AA-stacking. This interlayer decoupling also results in a notable increase (up to $\sim 25\text{-}50\%$) of the bandgap of twisted bilayers, with the valance band edge becoming relatively flat with van-Hove singularities in the density of states. Thus, hole doping induces a Stoner instability, leading to ferromagnetic ground state, which is more robust in Moiré superlattices, than that of AA-stacked β -P and β -As.

I. INTRODUCTION

The era of 2D materials started with the discovery of graphene, hosting massless Dirac quasiparticles, with gate tunable electronic and optical properties.¹⁻³ This motivated the discovery of several other 2D semiconductors. Among them, transition metal dichalcogenides (such as MoS_2 , WS_2 etc.)⁴⁻⁶ and black phosphorene^{7,8} are some of the predominantly explored candidates. Several useful applications including transistors based on graphene,^{9,10} MoS_2 ,¹¹ and black phosphorene¹² have already been demonstrated.¹³ There has also been significant interest in twisted bilayers forming Moiré superlattices, with the twist angle offering another handle on the tunability of electronic and optical properties.¹⁴⁻¹⁶ In particular, several recent studies on twisted bilayer graphene explore the presence of flat bands and the van-Hove singularities (vHs) resulting in exciting many body instabilities, on account of the relative rotation between the layers.¹⁷⁻²²

The properties of ultrathin layered materials are governed by the stacking sequence of the monolayers, which dictates the interlayer orbital overlap among different layers. Thus, understanding the influence of the stacking sequences on the nature of the interlayer interaction among monolayers has been of great fundamental interest.²³⁻²⁹ Motivated by this, in this paper we explore the nature of the interlayer coupling and the modulation of the electronic and magnetic properties in twisted bilayers of blue phosphorus (β -P)^{30,31} and grey arsenene (β -As),^{32,33} both having similar crystal structure and physical properties. Among several possible 2D allotropes predicted for group-V elements,³⁴ β -P has already been reported experimentally,^{35,36} along with a detailed atomistic study of its growth mechanism.³⁷ β -allotrope of group-V elements have a graphene like buckled honeycomb structure, as opposed to the puckered honeycomb

crystal of black phosphorene or α -P. In terms of electronic transport properties, both the allotropes are found to be comparable.³⁸ Interestingly, a hole doping induced ferromagnetic ground state has been reported in case of β -P.^{39,40}

Our study reveals that the p_z orbitals contribute significantly to the valance as well as conduction band edge of the bilayers of AA-stacked β -P and β -As. Thus, the interactions among the p_z orbitals on different layers are impacted significantly by the relative rotation of the layers relative to each other. We find that, increasing the rotation angle leads to larger interlayer distances and reduced binding energy in both β -As and β -P bilayers. As a result, the bandgap increases in Moiré superlattices, and also shows more modulation with applied electric field and strain. Additionally, the highest valance band of the Moiré superlattices also becomes relatively flat with van Hove singularities in the density of states. This leads to Stoner instability induced ferromagnetic ground state with hole doping, which is found to be more stable in twisted structures, than that of AA-stacked bilayers.

The manuscript is organized as follows: In Sec. II, we describe the details of the density functional theory (DFT) calculations. The electronic properties and the interlayer decoupling of the Moiré superlattice are discussed in detail in the Sec. III; in the context of binding energy, electronic band structure and its modulation with vertical electric field and strain, and magnetic instability in Moiré superlattices. The results are summarized in Sec. IV.

II. METHODOLOGY

Structural relaxations and electronic band structure calculations are performed using density functional theory (DFT), as implemented in the Quantum ESPRESSO package.⁴¹ A plane wave basis set with kinetic energy cut-

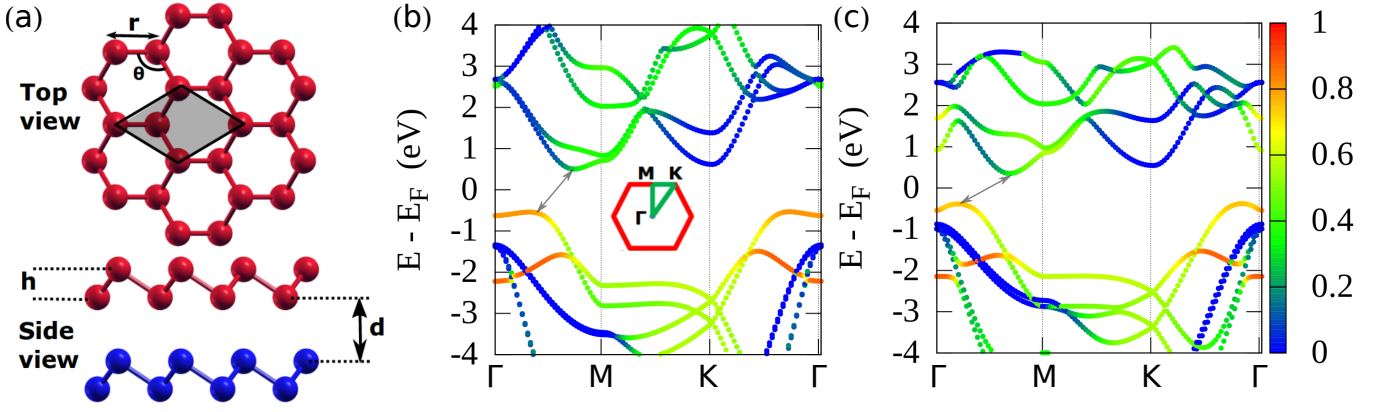


FIG. 1. (a) The crystal structure of bilayer β -P and β -As. On account of the AA-stacking, both the top (red) and bottom (blue) layer are visible separately in the side view only. The unit cell is highlighted in the top view. The Orbital resolved electronic band structures (plotted along the high symmetry lines shown in the inset) of bilayer β -P and β -As are illustrated in (b) and (c), respectively. The arrow connects the valence band maximum (VBM) and conduction band minimum (CBM). The color scale shows the relative weight of the p_z orbitals on different energy bands. Clearly, the p_z orbitals dominate near the VBM, and have significant contribution near the CBM as well.

off of 30 Ry and projector augmented wave pseudopotentials are used. Exchange-correlation effects are included within the framework of generalized gradient approximations (GGA), as proposed by Perdew-Burke-Ernzerhof (PBE).⁴² Dispersive forces are taken into account by using the vdW-DF-objk8 van der Waals correction.^{43–45} A k -point mesh of $24 \times 24 \times 1$ is used for Brillouin zone integrations in case of smaller unit cells of AA-stacked bilayers and a coarser mesh is chosen for the Moiré superlattices in twisted bilayers, according to their size. Structural optimizations are carried out until the energy difference between two successive steps of ionic relaxation are less than 10^{-4} Ry and all three components of the force on each atom belonging to the unit cell are less than 10^{-3} Ry/Bohr. A vacuum of 20 Å is applied perpendicular to the plane to avoid spurious interactions between the periodic replicas in the out-of-plane direction. The crystal structures are prepared by XCrysden software.⁴⁶

III. RESULTS AND DISCUSSIONS

A. AA-stacked bilayers: crystal and electronic band structure

The β -allotrope of monolayer P and As are known to have a buckled honeycomb structure.^{27,32,34,47} Among several possible stacking sequences, AA-stacked bi-layers are known to have the lowest energy configuration.^{27,47} The top and side view of the crystal are shown in Fig. 1(a). The values of the structural parameters marked in Fig. 1(a), like the bond length (r), bond angle (θ), buckling height (h) and interlayer separation (d), are reported in Table I. These are in good agreement with the earlier studies on β -P⁴⁷ (reported values of $r = 2.26$ Å, $\theta = 93.06^\circ$, $h = 1.24$ Å, $d = 3.23$ Å) and β -As²⁷ (re-

TABLE I. Structural parameters and bandgap of AA-stacked bilayer β -P and β -As. Our calculations are in good agreement with earlier works on β -P⁴⁷ and β -As²⁷ (see main text for details).

Crystal	r (Å)	θ	h (Å)	d (Å)	E_g (eV)
β -P	2.26	93.06°	1.24	3.35	1.17
β -As	2.51	92.14°	1.39	3.2	0.86

ported values of $r = 2.51$ Å, $\theta = 91.87^\circ$, $h = 1.4$ Å, $d = 3.27$ Å).

Surveying the structural data available in the literature for these bilayers, we find that the interlayer distance is sensitive to the choice of van der Waals interaction parameters, and values ranging from 3.23 to 3.40 Å [3.14 to 3.27 Å] are reported for AA-stacked β -P [β -As].^{27,47–49} Unlike the inter-layer distance, other structural parameters like unit cell dimension, bond length and bond angle are independent of the choice of the van der Waals interaction, and the reported values lie within a very narrow range.^{27,47–49} In our calculations, the interlayer distance lies within the range of values reported in the literature, and the other structural parameters match very closely (within 1-2%). This validates our choice of the pseudopotential and other calculation parameters like kinetic energy cut-off and k -point mesh used in this work.

The calculated electronic band structures of bilayer AA-stacked β -P and β -As are shown in Fig. 1(b) and Fig. 1(c), respectively. Evidently, both of them have similar qualitatively features: an indirect bandgap, with conduction band minimum (CBM) and valance band maximum (VBM) located at some point along the Γ M line. In the valence band, there is another point comparable to that of the VBM energy, lying in between the Γ K line. Relative weight of the p_z orbitals on different energy

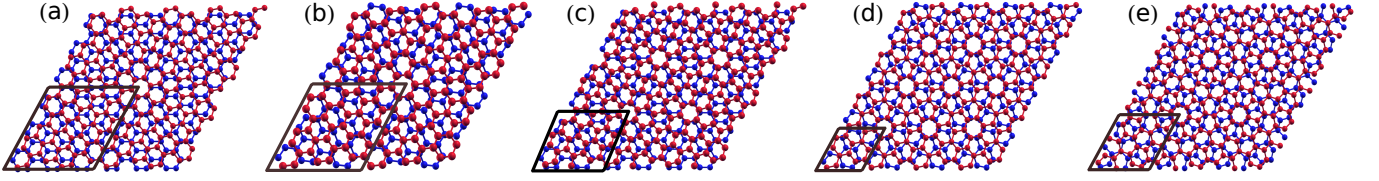


FIG. 2. Moiré superlattices of β -P and β -As (with a hexagonal unit cell), as obtained by rotating one layer with respect to the other by five different angles. Rotation angles (number of atoms per unit cell) in different panels are: (a) 10.9° (110), (b) 13.2° (72), (c) 16.1° (50), (d) 21.8° (28) and (e) 27.8° (52).

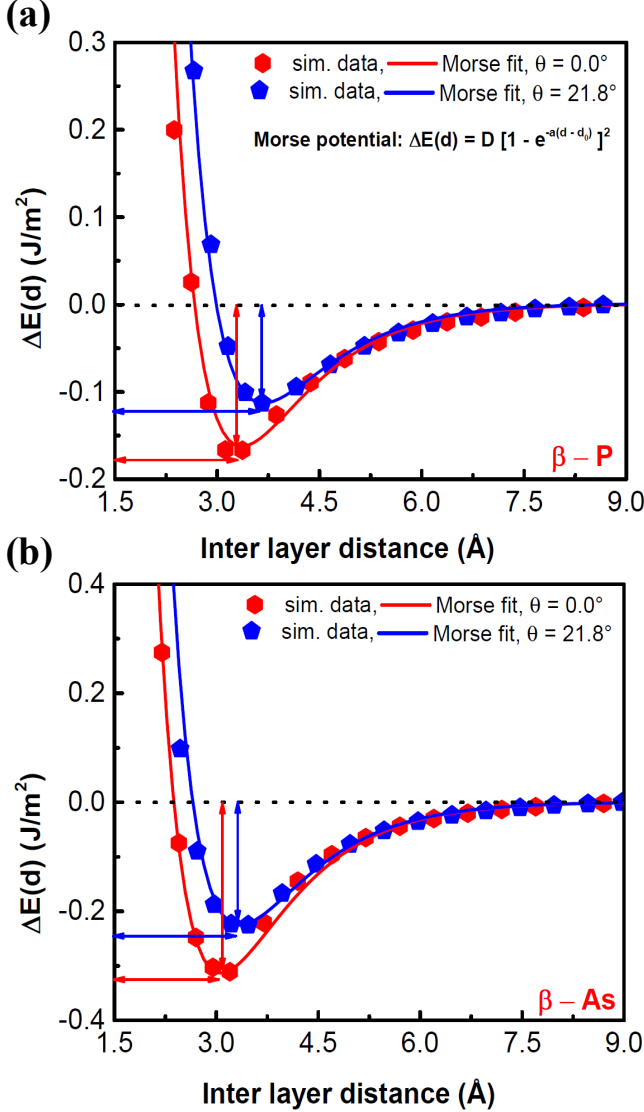


FIG. 3. Energy of bilayers per unit area (calculated with respect to energy of two “infinitely” separated monolayers) plotted as a function of the interlayer separation d for (a) β -P and (b) β -As. ΔE fits well to the Morse potential. The depth of the energy well represents the binding energy. In the case of both the allotropes, binding energy in twisted structures with Moiré pattern reduces by $\sim 33\%$, resulting in an increase in the interlayer distance of $\sim 10\%$.

bands clearly shows their dominance near the valence band edge. On the other hand, while p_z orbitals have notable contributions near the conduction band edge, p_x and p_y orbitals are found to have equally significant contributions. There is a large anisotropy in the band dispersion, in vicinity of both VBM and CBM. This will lead to highly anisotropic charge carrier effective mass, as reported in case of monolayer allotropes.^{34,38} The indirect bandgap values are reported in Table I, and they are in good agreement with the values reported in the literature.^{27,47} However, the bandgap in GGA based calculations are known to be underestimated, and nearly two fold increase is reported with use of more accurate hybrid functionals.^{27,47}

B. Binding energy

In case of layered materials, monolayers are believed to be stacked on top of each other and held together by Van der Waals (VDW) interactions. Such forces are isotropic in nature and bonding between two monolayers is expected to be independent of their relative orientation. This hypothesis is tested in case of twisted bilayers of β -P and β -As (forming Moiré patterns), by comparing their binding energies with that of AA-stacked bilayers. We use the optimized structures of AA-stacked bilayers to generate the Moiré superlattices of β -P and β -As, by rotating one layer with respect to the other. We select five rotation angles, namely, 10.9° , 13.2° , 16.1° , 21.8° and 27.8° . The Moiré superlattices for different relative rotation angles, each of them having a hexagonal unit cell, are shown in Fig. 2. Binding between two monolayers is characterized by calculating the difference between the energy of two “infinitely separated” monolayers and a bilayer with inter-layer separation d :

$$\Delta E_{DFT}(d) = \frac{E_{bilayer}(d) - 2 \times E_{monolayer}}{A}, \quad (1)$$

where A is the area of the unit cell and d is varied over a range from 2.5 to 9 Å, beyond which ΔE is found to be independent of d . In case of twisted bilayers with Moiré patterns, the interlayer distance d is calculated by first measuring the distance between an atom at layer 1 and its closest neighbor at layer 2 and then taking an average of the distances measured between all such pairs. The calculated values of $\Delta E_{DFT}(d)$ for AA stacked and

twisted bilayers are shown by the symbols in Fig. 3 (a) and (b) for β -P and β -As, respectively.

Further analysis is carried out by fitting the data points obtained from DFT calculations with a Morse potential, which is known to reasonably describe the non-bonded interlayer interactions, particularly at large d . The Morse potential is given by $\Delta E_{\text{Morse}}(d) = D [1 - e^{-a(d-d_0)}]^2$, where D is the potential depth, d_0 is the equilibrium separation and a (taken to be 1 in our case) controls the width of the potential. The potential depth or D , is the difference between the energies at equilibrium separation d_0 (equal to 3.35 and 3.2 Å for AA-stacked P and As) and at a large value of d , where there is no interaction between the monolayers. As shown in Fig. 3, this energy is almost constant for interlayer distance ~ 9 Å, and thus we will use 9 Å as the large d value to calculate D for the Morse fit. As shown in Fig. 3 (a)-(b), AA-stacked β -As has larger (0.30 J/m²) binding energy than that of β -P (0.16 J/m²). Same is true for the twisted structure with Moiré patterns, with β -As (0.21 J/m²) having nearly twice the binding energy than that of β -P (0.11 J/m²). Comparing with the AA-stacked bilayers, the binding energy decreases and interlayer separation increases in case of twisted structures.

The variation of interlayer distance and binding energy as a function of stacking sequence can be attributed to the steric effect: the repulsion between the overlapping electron clouds. Steric effect depends on the size and in-plane interatomic distance of the constituent atoms. For example, larger size and interatomic distance of S atom in MoS₂ compared to that of the C atom in graphene, results in a 3 times stronger steric effect in MoS₂.²⁵ Since P and As atoms are comparable in size with S atom, large steric effect is expected in case of β -P and β -As as well.

Indeed, bilayers of β -P and β -As show a wide range of interlayer distances and binding energies for different stacking sequences. The most stable ground-state stacking in the bilayers is the AA-configuration.^{27,28} The twisted bilayers with Moiré pattern can be considered to be a ‘‘mixture’’ of all possible stacking sequences. Thus the binding energy of the twisted structures is expected to be lower than that of AA-stacking. Our calculations reveal nearly 33% reduction of binding energy and 10% increase of interlayer separation in 21.8° rotated twisted structures, compared to AA-stacked bilayers. The large dependence of the binding energy on the orientation of the constituent monolayers, clearly highlights the role of steric effects in these bilayers. Thus the interlayer bonding in the bilayers of β -P and β -As is not purely of VDW type. Similar observation has also been reported for the other layered allotrope such as black phosphorus.²⁹

C. Electronic band structure of twisted bilayers

In the previous subsection, we showed that the formation of the Moiré patterns weakens the interlayer interaction. Increased interlayer distance in Moiré pattern

of β -P and β -As leads to the reduction in the overlap among out of the plane p_z orbitals. Since both valence band maximum (VBM) and conduction band minimum (CBM) have significant contributions from the p_z orbitals [see Fig. 1(b) and (c)], decreasing overlap among such orbitals is expected to have significant effects.

Two such band structures are shown for $\theta = 21.8^\circ$ rotated Moiré superlattice of β -P and β -As, in Fig. 4(a) and (b), respectively. Interestingly, for this particular rotation, both the bilayers are transformed to a direct bandgap semiconductor, with the valence and conduction band edges located in the middle of the Γ -M line. Note that, since the unit cells of the Moiré superlattices are also hexagonal, the high symmetry points in the reciprocal space are the same as in Fig. 1(b). The magnitude of the bandgap is plotted as a function of rotation angle θ in Fig. 4 (c) and (d), for β -P and β -As, respectively. As shown in the figures, compared to AA-stacked bilayers, bandgap in Moiré superlattices can increase up to $\sim 25\%$ and 50% in case of P and As, respectively. While the bandgap values fall within a relatively small window, ranging from 1.4 to 1.5 eV in case of β -P Moiré superlattices, it changes prominently as a function of θ in case of β -As, which opens the possibility of bandgap tuning in the latter, by rotating one layer relative to the other. In order to analyze the connection between bandgap magnitude and interlayer separation, we also plot the latter as a function of the rotation angle in Fig. 4 (c) and (d). Evidently, the bandgap enhancement is highly correlated with the increasing interlayer separation and the decreasing overlap among the p_z orbitals of adjacent layers.

Other than the $\theta = 21.8^\circ$, rest of the Moiré superlattices are indirect bandgap semiconductors as shown in Fig. 4(c) and (d). However, due to the flatness of the valence band, the difference between the direct and indirect bandgap is very small in most of the cases [see Fig. S1 and S2 in the Supporting Information]. The flatness of the bands in vicinity of the band edges also gives rise to a large density of states, which is conducive to magnetic and other many-body instabilities. A recent example is that of the ‘magic angle’ twisted bilayer graphene, which shows superconducting instability.^{18–21}

D. Band structure modulation with electric field

We now explore the possibility of bandgap engineering in these twisted bilayers by means of a vertical electric field. In case of β -P and β -As, very large electric field (about 0.5 V/Å) is known to reduce the bandgap, ultimately leading to an insulator to metal transition around 0.7 to 1 V/Å.^{32,47} Moreover, an interesting topological transformation is also reported for monolayer β -As, at nearly 1 V/Å electric field.³²

A similar trend is observed in case of Moiré superlattices, where bandgap magnitudes decrease sharply beyond 0.3 [0.4 V/Å] for bilayer β -P [β -As]. A comparison of bandgap modification (with increasing electric field

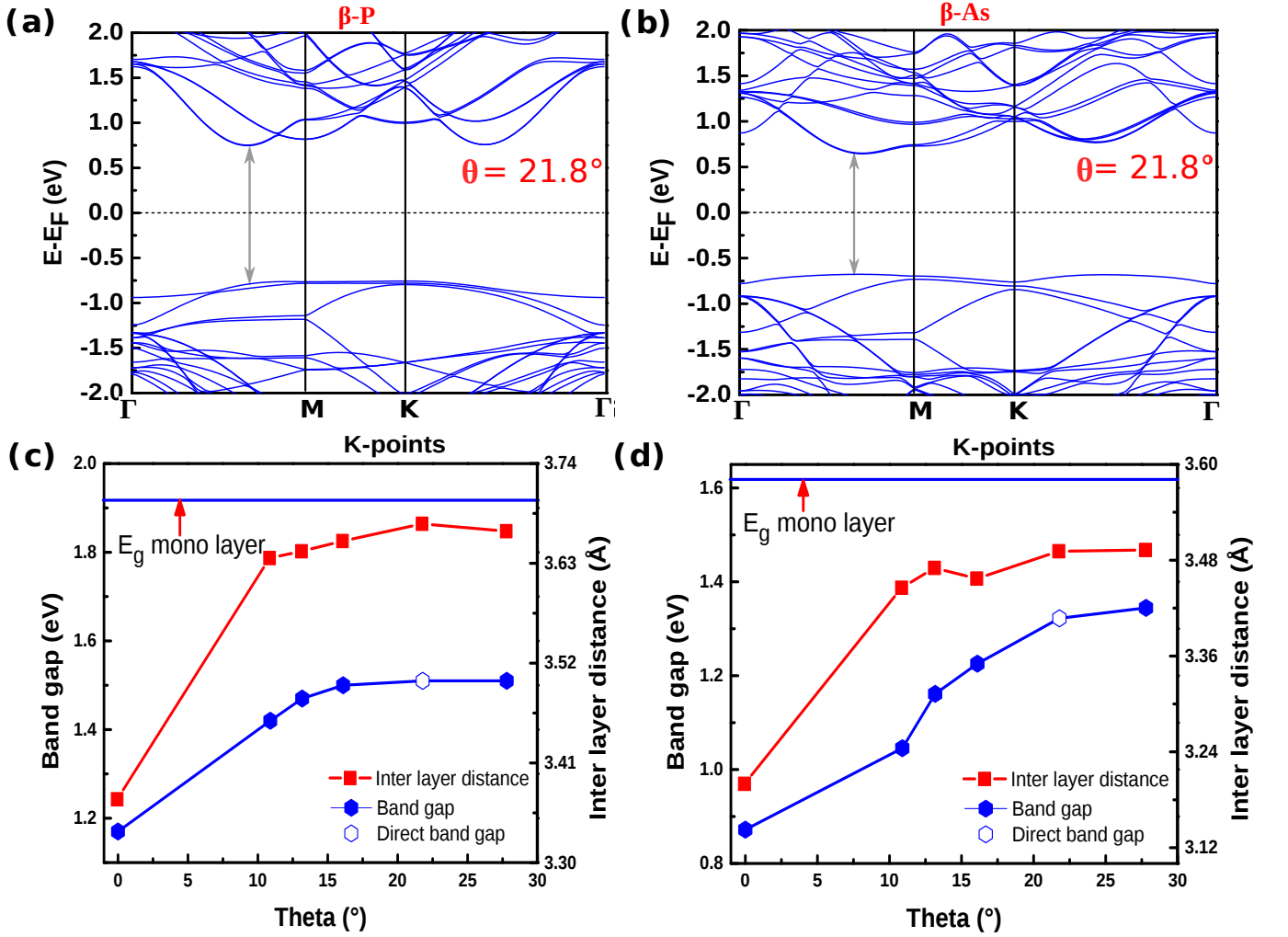


FIG. 4. Electronic band structure of 21.8° rotated Moiré pattern of bilayer (a) β -P and (b) β -As. For this particular rotation, both the bilayers are converted to a direct bandgap semiconductor, with both the valence and the conduction band edges located in the middle of the Γ -M line. The variation of the bandgap and the interlayer separation, as a function of the twist angle θ is shown in (c) β -P and (d) β -As. Clearly, there is a strong correlation between the bandgap and the interlayer separation of both the Moiré superlattices.

strength) in AA-stacked bilayers and Moiré superlattices is shown in Fig. 5 (a). Interestingly, the latter (originally a direct bandgap semiconductor) is found to be converted to an indirect bandgap semiconductor at high electric field, both in case of β -P and β -As. This transition happens because the conduction band edge is shifted to the Γ point (see Fig. S3 and S4 in SI). The computationally predicted electric field values of 0.3-0.4 V/Å can further be reduced if we account for the presence of ripples and other structural imperfections.⁵⁰

E. Band structure modulation with strain

Monolayers of β -P and β -As also show significant bandgap modulation under the influence of external strain.^{27,30,32} A similar trend is observed in case of AA-

stacked bilayers and Moiré superlattices of β -P and β -As. As shown in Fig. 5(b), the bandgap decreases monotonically under tensile strain. On the other hand, under compression, bandgap initially increases, followed by a decrease at higher value of strain. Evolution of electronic band structures as a function of strain for AA-stacked β -P and β -As are shown in SI (see Fig. S5 and S6). We find that, not only the magnitude of bandgap decreases under strain, band edges also shift from their original location. For example, in case of AA-stacked β -P, CBM and VBM shifts to the K-point and Γ -point at 2% and 4% compressive strain, respectively (see Fig. S5 in SI). On the other hand, in case of AA-stacked β -As, VBM moves to the Γ -point under 3% compressive strain, while CBM shifts to the Γ -point at 4% tensile strain (see Fig. S6 in SI). However, we do not find any indirect to direct bandgap conversion within $\pm 5\%$ strain in case of AA-stacked β -P

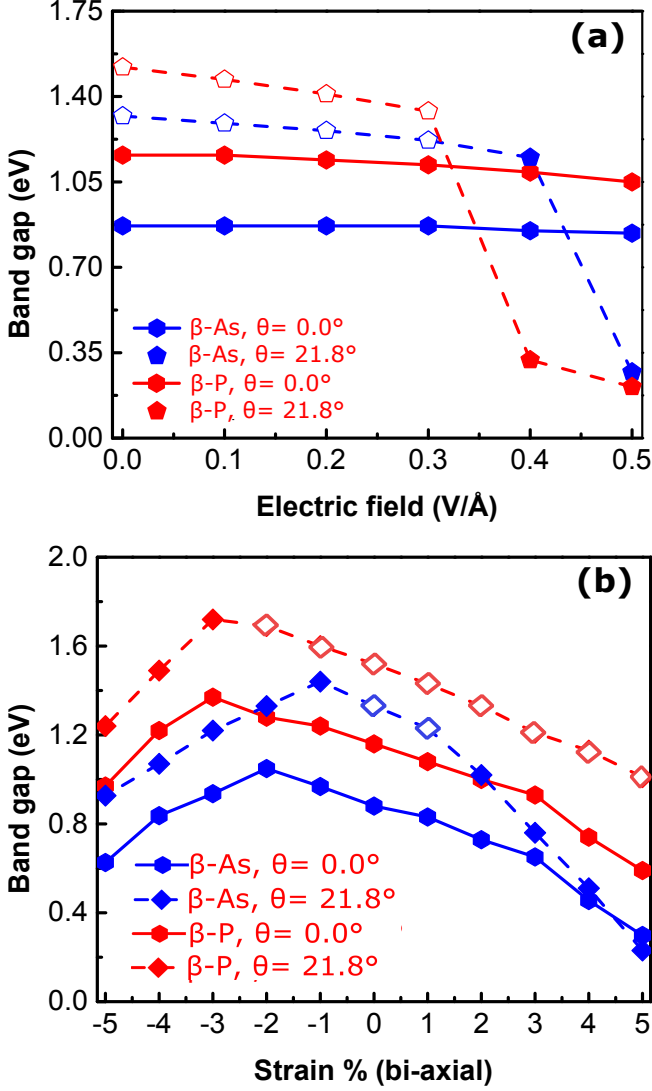


FIG. 5. (a) The evolution of the bandgap of bilayer β -P and β -As with the strength of a vertical electric field. The twisted structures with a larger interlayer separation are impacted more, as expected. (b) Bandgap engineering with bi-axial strain.

and β -As.

Interestingly, for Moiré superlattices, the bilayers can also convert from a direct to an indirect bandgap semiconductor under strain. This is more prominent in case of β -As Moiré superlattice ($\theta = 21.8^\circ$), which changes to an indirect bandgap semiconductor under relatively small tensile (2%), as well as compressive (1%) strain. On the other hand, β -P Moiré superlattice ($\theta = 21.8^\circ$) undergoes such a transition only under compression (3%). A detailed analysis reveals that the band edges shift to different valleys as a function of strain, leading to a direct to indirect bandgap transformation. For example, in case of β -P Moiré superlattice, the valence band edge moves to the Γ point and the conduction band edge moves to the K-point at 3% compression (see Fig. S7 in SI). On

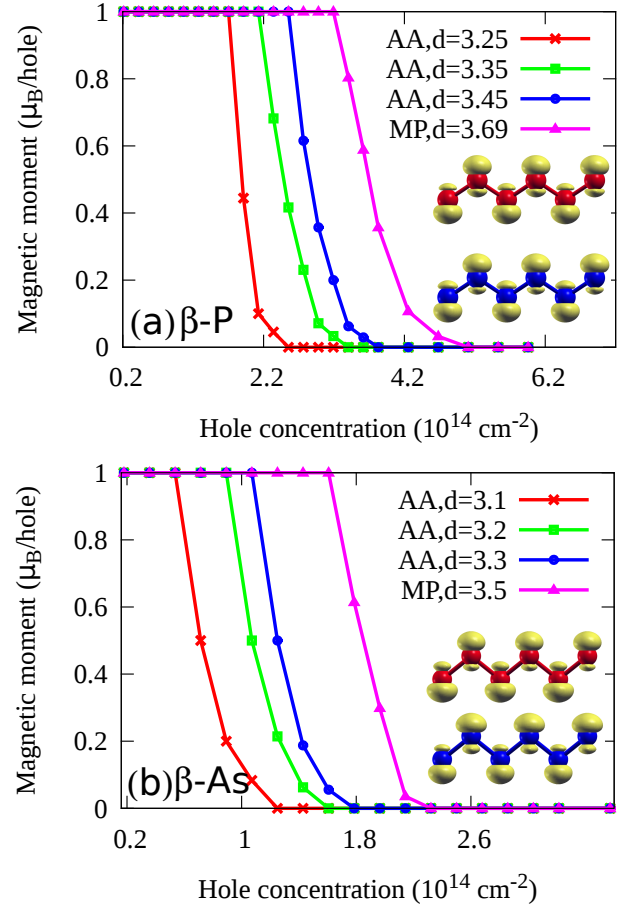


FIG. 6. Variation of magnetic moment as a function of hole concentration for AA-stacked bilayer (a) β -P and (b) β -As. The critical value of hole doping, up to which ferromagnetism exists, increases with interlayer distance d . The inset in both the panels, show the out of plane spin density. Clearly the major spin contribution is from the p_z orbitals of P and As atoms, whose interaction is d dependent. In case of Moiré super-lattice ($\theta = 21.8^\circ$) with larger d , the interlayer decoupling supports the ferromagnetic ground state up to higher doping concentration.

the other hand, in case of β -As Moiré superlattice, the valence band edge moves to the Γ point at 1% compressive strain, while a 2% tensile strain triggers a similar shift to the conduction band edge. (see Fig. S8 in SI).

F. Magnetic instability

As shown Fig. 1(b)-(c) and Fig. 4(a)-(b), the valence band of bilayer β -P and β -As have a relatively flat shape near the VBM. This results in a van Hove singularity in the electronic density of states near the valence band edge, which can be explored via hole doping. The van Hove singularity is conducive to quantum many body instabilities such as magnetism. In fact, magnetism arising

from the van Hove singularity induced Stoner instability in monolayers and bilayers of P and As has already been predicted over a broad range of hole doping.^{39,40}

Here we explore the existence of a ferromagnetic instability in hole doped bilayers of twisted β -P and β -As. The calculated magnetic moment (per hole) in the Ferromagnetic ground state is shown in Fig. 6. Our calculations reveal that the magnetic moment is equal to the number of holes in the system up to certain value of doping, beyond which both the bilayers fall back to the non-magnetic state rapidly. The critical value of hole concentration at which the crossover takes place is nearly double in AA-stacked β -P, than that of β -As. This is in good agreement with the reported data in the literature.^{39,40} Note that, prediction of a ferromagnetic ground state up to 10^{14} cm⁻² hole concentration is very encouraging, because it is within the range of current experimental capabilities, as demonstrated for gate-tunable MoS₂ device.⁵¹

As shown in the respective insets for Fig. 6, the spin density is predominantly localized in the p_z orbitals of the P and As atoms. Thus, the increase in the interaction of the p_z orbitals with decreasing interlayer separation in bilayers is likely to result in the weakening of the magnetic ground state. This is confirmed by calculating the magnetic moment by changing the interlayer separation d (slightly above and below the equilibrium value) for AA-stacked bilayers in Fig. 6. As expected we find that the critical value of hole doping, up to which the AA-stacked bilayers remain in ferromagnetic ground state, gradually decreases as the monolayers are brought closer to each other. This is also reflected in the fact that the ferromagnetic ground state survives up to higher hole concentration in case of Moiré superlattices (see Fig. 6 for results for $\theta = 21.8^\circ$), which has a larger interlayer distance and smaller interactions among the p_z orbitals. In fact, the ferromagnetic ground state can exist up to nearly 50% higher hole doping in Moiré superlattices as compared to the AA-stacked bilayers, making the former more suitable for magnetic and spintronic applications.

IV. CONCLUSION

In conclusion, we have investigated the evolution of interlayer coupling in twisted β -P and β -As bilayers. Our

calculations reveal nearly 33% reduction in binding energy, leading to 10% increase of interlayer separation in Moiré superlattices of β -P and β -As, compared to AA-stacked bilayers. We show that the band edges (particularly the VBM) are dominated by the out of plane p_z orbitals in both β -P and β -As. Thus, increasing the interlayer separation reduces the overlap among p_z orbitals from adjacent planes. This interlayer decoupling in Moiré superlattices leads to significant changes in the electronic, as well as magnetic (with hole doping) properties of β -P and β -As.

We have shown that compared to AA-stacked bilayers, bandgap increases by 25-50% in Moiré superlattices. Furthermore, on account of a relatively flat valence band, the difference between the direct and indirect bandgap is very small. In some cases, twisted bilayers are found to be direct bandgap semiconductors, while the AA-stacked bilayers are indirect bandgap semiconductors. Similar to other 2D materials, bandgap can be tuned by applying strain, as well as an electric field normal to the plane of the twisted bilayers.

Due to the Stoner instability originating from the van Hove singularity of density of states near the valence band edge, a ferromagnetic ground state is observed in bilayer β -P and β -As. The critical value of hole concentration, up to which the ferromagnetic ground state is sustained, increases by $\sim 50\%$ in Moiré superlattices, compared to AA-stacked bilayers. Thus, twisted bilayers are better candidates than AA-stacked β -P and β -As for the purpose of magnetic and spintronic applications.

V. ACKNOWLEDGMENTS

The authors acknowledge funding from the Ramanujan fellowship research grant, the DST Nanomission project and SERB (EMR/2017/004970). The authors also thank the computer center of IIT Kanpur for providing HPC facility.

* bsomnath@iitk.ac.in

¹ A. K. Geim and K. S. Novoselov, "The rise of graphene," *Nat. Mater.* **6**, 183–191 (2007)

² A. H. Castro Neto, F. Guinea, N. M. R. Peres, K. S. Novoselov, and A. K. Geim, "The electronic properties of graphene," *Rev. Mod. Phys.* **81**, 109–162 (2009)

³ Yujia Zhong, Zhen Zhen, and Hongwei Zhu, "Graphene: Fundamental research and potential applications," *FlatChem* **4**, 20 – 32 (2017)

⁴ Manish Chhowalla, Hyeon Suk Shin, Goki Eda, Lain-Jong Li, Kian Ping Loh, and Hua Zhang, "The chemistry of two-dimensional layered transition metal dichalcogenide nanosheets," *Nat. Chem.* **5**, 263 (2013)

⁵ Xiaodong Xu, Wang Yao, Di Xiao, and Tony F. Heinz, "Spin and pseudospins in layered transition metal dichalcogenides," *Nat. Phys.* **10**, 343 (2014)

⁶ Juan Xia, Jiayu Yan, and Ze Xiang Shen, "Transition metal dichalcogenides: structural, optical and electronic property tuning via thickness and stacking," *FlatChem* **4**,

- 1 – 19 (2017)
- ⁷ Han Liu, Adam T. Neal, Zhen Zhu, Xianfan Xu, David Tomnek, and Peide D. Ye, “Phosphorene: An unexplored 2d semiconductor with a high hole mobility,” *ACS Nano* **8**, 4033–4041 (2014)
- ⁸ Shenghuang Lin, Yingsan Chui, Yanyong Li, and Shu Ping Lau, “Liquid-phase exfoliation of black phosphorus and its applications,” *FlatChem* **2**, 15 – 37 (2017)
- ⁹ Frank Schwierz, “Graphene transistors,” *Nat. Nanotechnol.* **5**, 487 (2010)
- ¹⁰ Jihyun Paek, Joohee Kim, Byeong Wan An, Jihun Park, Sangyoon Ji, So-Yun Kim, Jiuk Jang, Youngjin Lee, Young-Geun Park, Eunjin Cho, Subin Jo, Seoyeong Ju, Woon Hyung Cheong, and Jang-Ung Park, “Stretchable electronic devices using graphene and its hybrid nanostructures,” *FlatChem* **3**, 71 – 91 (2017)
- ¹¹ B. Radisavljevic, A. Radenovic, J. Brivio, V. Giacometti, and A. Kis, “Single-layer Mos2 transistors,” *Nat. Nanotechnol.* **6**, 147 (2011)
- ¹² Likai Li, Yijun Yu, Guo Jun Ye, Qingqin Ge, Xuedong Ou, Hua Wu, Donglai Feng, Xian Hui Chen, and Yuanbo Zhang, “Black phosphorus field-effect transistors,” *Nat. nano.* **9**, 372 (2014)
- ¹³ Jun Dai and Xiao Cheng Zeng, “Bilayer phosphorene: Effect of stacking order on bandgap and its potential applications in thin-film solar cells,” *J. Phys. Chem. Lett.* **5**, 1289–1293 (2014)
- ¹⁴ Qingjun Tong, Hongyi Yu, Qizhong Zhu, Yong Wang, Xiaodong Xu, and Wang Yao, “Topological mosaics in moiré superlattices of van der waals heterobilayers,” *Nature Physics* **13**, 356 (2016)
- ¹⁵ Kyoungwan Kim, Ashley DaSilva, Shengqiang Huang, Babak Fallahazad, Stefano Larentis, Takashi Taniguchi, Kenji Watanabe, Brian J. LeRoy, Allan H. MacDonald, and Emanuel Tutuc, “Tunable moiré bands and strong correlations in small-twist-angle bilayer graphene,” *Proceedings of the National Academy of Sciences* **114**, 3364–3369 (2017)
- ¹⁶ Yuan Cao, Valla Fatemi, Shiang Fang, Kenji Watanabe, Takashi Taniguchi, Efthimios Kaxiras, and Pablo Jarillo-Herrero, “Unconventional superconductivity in magic-angle graphene superlattices,” *Nature* **556**, 43 (2018)
- ¹⁷ Zhenjun Tan, Jianbo Yin, Cheng Chen, Huan Wang, Li Lin, Luzhao Sun, Jinxiong Wu, Xiao Sun, Haifeng Yang, Yulin Chen, Hailin Peng, and Zhongfan Liu, “Building large-domain twisted bilayer graphene with van hove singularity,” *ACS Nano* **10**, 6725–6730 (2016), <https://doi.org/10.1021/acsnano.6b02046>
- ¹⁸ J. M. B. Lopes dos Santos, N. M. R. Peres, and A. H. Castro Neto, “Graphene bilayer with a twist: Electronic structure,” *Phys. Rev. Lett.* **99**, 256802 (2007)
- ¹⁹ Guohong Li, A. Luican, J. M. B. Lopes dos Santos, A. H. Castro Neto, A. Reina, J. Kong, and E. Y. Andrei, “Observation of van hove singularities in twisted graphene layers,” *Nature Physics* **6**, 109 (2009)
- ²⁰ I. Brihuega, P. Mallet, H. González-Herrero, G. Trambly de Laissardière, M. M. Ugeda, L. Magaud, J. M. Gómez-Rodríguez, F. Ynduráin, and J.-Y. Veuillen, “Unraveling the intrinsic and robust nature of van hove singularities in twisted bilayer graphene by scanning tunneling microscopy and theoretical analysis,” *Phys. Rev. Lett.* **109**, 196802 (2012)
- ²¹ Wei Yan, Mengxi Liu, Rui-Fen Dou, Lan Meng, Lei Feng, Zhao-Dong Chu, Yanfeng Zhang, Zhongfan Liu, Jia-Cai Nie, and Lin He, “Angle-dependent van hove singularities in a slightly twisted graphene bilayer,” *Phys. Rev. Lett.* **109**, 126801 (2012)
- ²² Bikash Padhi, Chandan Setty, and Philip W. Phillips, “Doped twisted bilayer graphene near magic angles: Proximity to wigner crystallization, not mott insulation,” *Nano Letters* **18**, 6175–6180 (2018), <https://doi.org/10.1021/acs.nanolett.8b02033>
- ²³ Jinglei Ping and Michael S. Fuhrer, “Layer number and stacking sequence imaging of few-layer graphene by transmission electron microscopy,” *Nano Letters* **12**, 4635–4641 (2012)
- ²⁴ Julia Berashevich and Tapash Chakraborty, “On the nature of interlayer interactions in a system of two graphene fragments,” *The Journal of Physical Chemistry C* **115**, 24666–24673 (2011)
- ²⁵ K. Liu, L. Zhang, T. Cao, C. Jin, D. Qiu, Q. Zhou, A. Zettl, P. Yang, S. G. Louie, and F. Wang, “Evolution of interlayer coupling in twisted molybdenum disulfide bilayers,” *Nature Communications* **5**, 4966 (2014)
- ²⁶ Jiaxu Yan, Juan Xia, Xingli Wang, Lei Liu, Jer-Lai Kuo, Beng Kang Tay, Shoushun Chen, Wu Zhou, Zheng Liu, and Ze Xiang Shen, “Stacking-dependent interlayer coupling in trilayer mos2 with broken inversion symmetry,” *Nano Letters* **15**, 8155–8161 (2015)
- ²⁷ D. Kecik, E. Durgun, and S. Ciraci, “Stability of single-layer and multilayer arsenene and their mechanical and electronic properties,” *Phys. Rev. B* **94**, 205409 (2016)
- ²⁸ Tian Zhang, Jia-He Lin, Yan-Mei Yu, Xiang-Rong Chen, and Wu-Ming Liu, “Stacked bilayer phosphorene: strain-induced quantum spin hall state and optical measurement,” *Scientific Reports* **5**, 13927 (2015), article
- ²⁹ L. Shulenburger, A.D. Baczewski, Z. Zhu, J. Guan, and D. Tomnek, “The nature of the interlayer interaction in bulk and few-layer phosphorus,” *Nano Letters* **15**, 8170–8175 (2015)
- ³⁰ Zhen Zhu and David Tománek, “Semiconducting layered blue phosphorus: A computational study,” *Phys. Rev. Lett.* **112**, 176802 (2014)
- ³¹ Jie Guan, Zhen Zhu, and David Tománek, “Phase coexistence and metal-insulator transition in few-layer phosphorene: A computational study,” *Phys. Rev. Lett.* **113**, 046804 (2014)
- ³² Sougata Mardanya, Vinay Kumar Thakur, Somnath Bhowmick, and Amit Agarwal, “Four allotropes of semiconducting layered arsenic that switch into a topological insulator via an electric field: Computational study,” *Phys. Rev. B* **94**, 035423 (2016)
- ³³ C. Kamal and Motohiko Ezawa, “Arsenene: Two-dimensional buckled and puckered honeycomb arsenic systems,” *Phys. Rev. B* **91**, 085423 (2015)
- ³⁴ Suhas Nahas, Akash Bajaj, and Somnath Bhowmick, “Polymorphs of two dimensional phosphorus and arsenic: insight from an evolutionary search,” *Phys. Chem. Chem. Phys.* **19**, 11282–11288 (2017)
- ³⁵ Jia Lin Zhang, Songtao Zhao, Cheng Han, Zhunzhun Wang, Shu Zhong, Shuo Sun, Rui Guo, Xiong Zhou, Cheng Ding Gu, Kai Di Yuan, Zhenyu Li, and Wei Chen, “Epitaxial growth of single layer blue phosphorus: A new phase of two-dimensional phosphorus,” *Nano Lett.* **16**, 4903–4908 (2016)
- ³⁶ Chengding Gu, Songtao Zhao, Jia Lin Zhang, Shuo Sun, Kaidi Yuan, Zehua Hu, Cheng Han, Zhirui Ma, Li Wang, Fengwei Huo, Wei Huang, Zhenyu Li, and Wei Chen,

- “Growth of quasi-free-standing single-layer blue phosphorus on tellurium monolayer functionalized au(111),” *ACS Nano* **11**, 4943–4949 (2017)
- ³⁷ Nannan Han, Nan Gao, and Jijun Zhao, “Initial growth mechanism of blue phosphorene on au(111) surface,” *J. Phys. Chem. C* **121**, 17893–17899 (2017)
- ³⁸ Achintya Priyadarshi, Yogesh Singh Chauhan, Somnath Bhowmick, and Amit Agarwal, “Strain-tunable charge carrier mobility of atomically thin phosphorus allotropes,” *Phys. Rev. B* **97**, 115434 (2018)
- ³⁹ Botao Fu, Wanxiang Feng, Xiaodong Zhou, and Yugui Yao, “Effects of hole doping and strain on magnetism in buckled phosphorene and arsenene,” *2D Materials* **4**, 025107 (2017)
- ⁴⁰ Xiaodong Zhou, Wanxiang Feng, Fei Li, and Yugui Yao, “Large magneto-optical effects in hole-doped blue phosphorene and gray arsenene,” *Nanoscale* **9**, 17405–17414 (2017)
- ⁴¹ Paolo Giannozzi, Stefano Baroni, Nicola Bonini, Matteo Calandra, Roberto Car, Carlo Cavazzoni, Davide Ceresoli, Guido L Chiarotti, Matteo Cococcioni, Ismaila Dabo, Andrea Dal Corso, Stefano de Gironcoli, Stefano Fabris, Guido Fratesi, Ralph Gebauer, Uwe Gerstmann, Christos Gougoussis, Anton Kokalj, Michele Lazzeri, Layla Martin-Samos, Nicola Marzari, Francesco Mauri, Riccardo Mazzarello, Stefano Paolini, Alfredo Pasquarello, Lorenzo Paulatto, Carlo Sbraccia, Sandro Scandolo, Gabriele Sclauszero, Ari P Seitsonen, Alexander Smogunov, Paolo Umari, and Renata M Wentzcovitch, “Quantum espresso: a modular and open-source software project for quantum simulations of materials,” *Journal of Physics: Condensed Matter* **21**, 395502 (2009)
- ⁴² John P. Perdew, Kieron Burke, and Matthias Ernzerhof, “Generalized gradient approximation made simple,” *Phys. Rev. Lett.* **77**, 3865–3868 (1996)
- ⁴³ T. Thonhauser, S. Zuluaga, C. A. Arter, K. Berland, E. Schröder, and P. Hyldgaard, “Spin signature of nonlocal correlation binding in metal-organic frameworks,” *Phys. Rev. Lett.* **115**, 136402 (2015)
- ⁴⁴ T. Thonhauser, Valentino R. Cooper, Shen Li, Aaron Puzder, Per Hyldgaard, and David C. Langreth, “Van der waals density functional: Self-consistent potential and the nature of the van der waals bond,” *Phys. Rev. B* **76**, 125112 (2007)
- ⁴⁵ D C Langreth, B I Lundqvist, S D Chakarova-Kck, V R Cooper, M Dion, P Hyldgaard, A Kelkkanen, J Kleis, Lingzhu Kong, Shen Li, P G Moses, E Murray, A Puzder, H Rydberg, E Schrder, and T Thonhauser, “A density functional for sparse matter,” *Journal of Physics: Condensed Matter* **21**, 084203 (2009)
- ⁴⁶ Anton Kokalj, “Computer graphics and graphical user interfaces as tools in simulations of matter at the atomic scale,” *Com. Mater. Sci.* **28**, 155–168 (2003)
- ⁴⁷ Barun Ghosh, Suhas Nahas, Somnath Bhowmick, and Amit Agarwal, “Electric field induced gap modification in ultrathin blue phosphorus,” *Phys. Rev. B* **91**, 115433 (2015)
- ⁴⁸ Renato B. Pontes, Roberto H. Miwa, Antônio J. R. da Silva, Adalberto Fazzio, and José E. Padilha, “Layer-dependent band alignment of few layers of blue phosphorus and their van der waals heterostructures with graphene,” *Phys. Rev. B* **97**, 235419 (2018)
- ⁴⁹ D. Kekic, E. Durgun, and S. Ciraci, “Optical properties of single-layer and bilayer arsenene phases,” *Phys. Rev. B* **94**, 205410 (2016)
- ⁵⁰ Shantanu Agnihotri, Priyank Rastogi, Yogesh Singh Chauhan, Amit Agarwal, and Somnath Bhowmick, “Significant enhancement of the stark effect in rippled monolayer blue phosphorus,” *J. Phys. Chem. C* **122**, 5171–5177 (2018)
- ⁵¹ J. T. Ye, Y. J. Zhang, R. Akashi, M. S. Bahramy, R. Arita, and Y. Iwasa, “Superconducting dome in a gate-tuned band insulator,” *Science* **338**, 1193–1196 (2012)